Hindawi Publishing Corporation
EURASIP Journal on Advances in Signal Processing
Volume 2008, Article ID 597613, 13 pages
doi:10.1155/2008/597613

Research Article

Multiple Interference Cancellation Performance for GPS Receivers with Dual-Polarized Antenna Arrays

Jing Wang and Moeness G. Amin

Center for Advanced Communications, College of Engineering, Villanova University, Villanova, PA 19085, USA

Correspondence should be addressed to Moeness G. Amin, moeness@ece.villanova.edu

Received 21 June 2007; Revised 31 March 2008; Accepted 25 June 2008

Recommended by Kostas Berberidis

This paper examines the interference cancellation performance in global positioning system (GPS) receivers equipped with dual-polarized antenna arrays. In dense jamming environment, different types of interferers can be mitigated by the dual-polarized antennas, either acting individually or in conjunction with other receiver antennas. We apply minimum variance distorntionless response (MVDR) method to a uniform circular dual-polarized antenna array. The MVDR beamformer is constructed for each satellite. Analysis of the eigenstructures of the covariance matrix and the corresponding weight vector polarization characteristics are provided. Depending on the number of jammers and jammer polarizations, the array chooses to expend its degrees of freedom to counter the jammer polarization or/and use phase coherence to form jammer spatial nulls. Results of interference cancellations demonstrate that applying multiple MVDR beamformers, each for one satellite, has a superior cancellation performance compared to using only one MVDR beamformer for all satellites in the field of view.

1. INTRODUCTION

GPS is a satellite navigation system used in localization, navigation, tracking, mapping, and timing [1]. At least four GPS satellites are necessary to compute the accurate positions in three dimensions and the time offset in the receiver clock. GPS signals are transmitted using direct sequence spread spectrum (DSSS) modulation with either coarse/acquisition (C/A) code on L1 band at 1575.42 MHz or precision (P) code on L2 band at 1227.6 MHz. Since GPS signals at the receivers are relatively weak (typically −20 dB below noise), interference is likely to degrade GPS performance and the code synchronization process. Several techniques have been developed to suppress, or at least, mitigate natural and man-made interferers. These techniques include temporal processing [2–5], spectral-based processing [6–8], subspace projection [9–11], and spatial signal processing [12–18]. Combinations of these techniques, such as time-frequency processing [19] and space-time processing [20–23], provide superior jammer suppression compared to single antenna and/or single domain processing.

The two methods of minimum variance distorntionless response (MVDR) and power inversion (PI) are commonly employed for adaptive antenna arrays to achieve desirable levels of interference cancellation. The MVDR beamformer cancels the interference without compromising the desired signals [15]. It adaptively places nulls toward the interference, while maintaining unit gains toward the direction of arrivals (DOAs) of the GPS satellites. This method has high-computation complexity and relies highly on prior and accurate knowledge of the DOAs of the desired signals which may be difficult to obtain at the "cold" start. Furthermore, if a jammer is closely aligned with one of the GPS satellites, the MVDR will retain both the GPS signal and the jammer strength, resulting in significant problems in signal acquisition and tracking. The PI method, on the other hand, suppresses interference by placing nulls toward high-power signals [12, 17, 18], hence mitigating jammers without prior knowledge of DOAs of the GPS signals. However, since DOAs of the satellites are not taken into considerations when forming the array response nulls, GPS signals can be subject to considerable attenuation.

Signal polarization can be effectively utilized to cancel different classes of jammers. A dual-polarized GPS antenna array aims at suppressing the RHCP, left-hand circular polarized (LHCP), and linearly polarized jammers, while

preserving the RHCP GPS signals. It is noted that an LHCP interference is immediately removed when using RHCP antennas. Further, a linearly polarized interference can be easily mitigated when the corresponding antenna weights are set to zero.

This paper considers an adaptive multiple MVDR beamforming applied to GPS receivers with dual-polarized antenna arrays. The spatial nulling and polarization properties are combined to obtain a superior interference cancellation performance for multiple jammers with distinct polarizations. Unlike single MVDR method, which employs one set of weights to satisfy unit-gain constraints toward all satellites, the multiple MVDR beamforming technique generates multiple beams, each corresponding to one GPS satellite. This method demonstrates excellent performance in dense jamming environments, and provides accurate tracking acquisition, even when a jammer is close to or aligned in angle with one of the GPS satellites [24]. The weights of each beamformer can be obtained using the least mean square (LMS) algorithm or other adaptive gradient algorithms. In this paper, we consider a GPS receiver equipped with dual-polarized uniform circular array (UCA), and use the constraint LMS algorithm to update the 2D beamformer weight vectors. The LMS algorithm can be applied in baseband or intermediate frequency (IF), and if needed, weights can be adjusted using analog adaptive loops [25].

Analysis of the eigenstructure of the covariance matrix and the corresponding weight vector polarization characteristics are provided. It is shown that, depending on the jammer number and polarizations, the array chooses to expend its degrees of freedom to effectively counter jammer polarization or/and form spatial nulls.

The paper begins with a description of the dual-polarized GPS receiver model. The adaptive MVDR algorithm is discussed, followed by simulations demonstrating its performance in a dense jamming environment. The simulation results show that the combination of the multiple MVDR technique and the dual-polarized antenna array improves the interference mitigation performance, compared with the single MVDR technique. Conclusions and observations are summarized at the end of the paper.

2. SYSTEM MODEL

2.1. Polarization concepts

The polarization of an electromagnetic wave is defined as the orientation of the electric field vector. The wave is composed of two orthogonal elements, E_X, which is received by the horizontal element of the antenna, and E_Y, which is received by the vertical element of the antenna. When the sum of the electric field vector E_X and E_Y oscillates on a straight line, the wave is linearly polarized, and when E_X and E_Y are of equal magnitude and 90 degrees out of phase as the sum of the electric field rotates around a circumference, the wave is referred to as circularly polarized. The direction of the rotation determines the polarization of the wave. Specifically, if the electric vector rotates counterclockwise, or the horizontal electric field vector is 90 degrees ahead of the vertical electric field vector, the wave is RHCP, otherwise, it is LHCP.

Define the unit vector at the horizontal direction as $\hat{x}$ and the unit vector at the vertical direction as $\hat{y}$. Accordingly, the signal arrival can be separated into a vertical component and a horizontal component. The normalized vector for a horizontally polarized signal can be denoted as

$$\begin{bmatrix} E_X & E_Y \end{bmatrix} = \begin{bmatrix} \hat{x} & 0 \end{bmatrix}, \tag{1}$$

and the normalized vector for the vertically polarized signal can be expressed as

$$\begin{bmatrix} E_X & E_Y \end{bmatrix} = \begin{bmatrix} 0 & -j\hat{y} \end{bmatrix}. \tag{2}$$

The normalized vector for the RHCP signal is represented as

$$\begin{bmatrix} E_X & E_Y \end{bmatrix} = \begin{bmatrix} \hat{x} & -j\hat{y} \end{bmatrix}, \tag{3}$$

and that for the LHCP signal is given by

$$\begin{bmatrix} E_X & E_Y \end{bmatrix} = \begin{bmatrix} \hat{x} & j\hat{y} \end{bmatrix}. \tag{4}$$

A dual-polarized antenna can be RHCP, LHCP, or linearly polarized. For a dual-polarized receiver antenna, the horizontal and the vertical antenna elements are allocated separate weights. The two weights can be organized to enforce certain polarization properties of individual antennas, or of the antenna array. For example, if the phase of the horizontal weight is 90 degrees ahead of that of the vertical weight, the antenna is RHCP. Similarly, if the phase is 90 degrees behind that of the vertical weight, the antenna is LHCP. If the vertical weight is zero, the antenna is horizontally polarized, whereas if the horizontal weight is zero, it is a vertically polarized antenna. If we assume zero coupling between the horizontal and vertical polarized signal components, then an RHCP antenna will provide the maximum signal power when receiving an RHCP signal, zero output when receiving an LHCP signal, and 3 dB attenuated signal when receiving a linearly polarized signal.

2.2. Block diagram of the GPS receiver

The block diagram of an N dual-polarized antenna array at the GPS receiver is depicted in Figure 1. At each antenna, two received signals corresponding to the vertical and horizontal polarizations are collected. In baseband processing, the output is the linear combination of the received inphase and quadrature signals processed by the corresponding complex weights.

The kth data samples received at the horizontal element and the vertical element of the ith antenna are denoted as $x_{iH}(k)$ and $x_{iV}(k)$, respectively. Thus, the $2N$-by-1 dual-polarized data vector $\mathbf{x}(\mathrm{k})$ is given by

$$\mathbf{x}(k) = \left[x_{1H}(k), x_{1V}(k), \ldots, x_{NH}(k), x_{NV}(k)\right]^T, \tag{5}$$

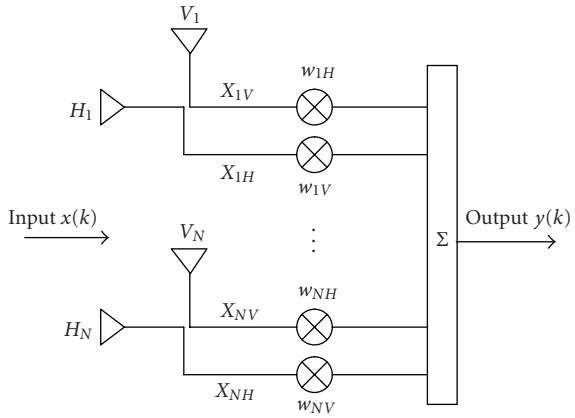

Figure 1: Block diagram of the dual-polarized antenna array receiver.

where $(\cdot)^T$ denotes transpose. Denote the $2N$-by-1 complex beamformer weight vector of the N dual-polarized antennas as

$$\mathbf{w} = \begin{bmatrix} w_{1H} & w_{1V} & w_{2H} & w_{2V} & \cdots & w_{NH} & w_{NV} \end{bmatrix}^T. \quad (6)$$

The corresponding antenna array output y(k) at the antenna array is given by

$$y(k) = \mathbf{w}^H \mathbf{x}(k), \quad (7)$$

where $(\cdot)^H$ denotes Hermition. Assume N dual-polarized antennas uniformly distributed on the circumference of a circle of radius d. Consider D GPS signals incident on the array from elevation angles $\theta_1, \theta_2, \ldots, \theta_D$ and azimuth angles $\varphi_1, \varphi_2, \ldots, \varphi_D$, respectively, and M narrowband interferers arrive at the array from elevation angles $\rho_1, \rho_2, \ldots, \rho_M$ and azimuth angles $\Phi_1, \Phi_2, \ldots, \Phi_M$, respectively. Assume the channel is an additive white Gaussian noise (AWGN) channel, and the GPS signal is a direct line-of-sight signal with no reflection or diffraction components.

Let a D-by-1 vector $\mathbf{s}_D(k)$ denotes the D complex GPS signals at the kth sample:

$$\mathbf{s}_D(k) = \left[s_1(k), s_2(k), ..., s_D(k)\right]^T. \quad (8)$$

Similarly, the M-by-1 interference vector $\mathbf{i}_M(k)$ represents the M complex interferers at the kth sample:

$$\mathbf{i}_M(k) = \left[i_1(k), i_2(k), \ldots, i_M(k)\right]^T. \quad (9)$$

Let $\mathbf{A}_D(\theta, \varphi)$ denote the $2N$-by-D steering matrix of the GPS signal:

$$\mathbf{A}_D(\theta, \varphi) = \begin{bmatrix} \mathbf{a}(\theta_1, \varphi_1) & \mathbf{a}(\theta_2, \varphi_2) & \cdots & \mathbf{a}(\theta_D, \varphi_D) \end{bmatrix}, \quad (10)$$

where $\mathbf{a}(\theta_i, \varphi_i)$ is the $2N$-by-1 steering vector of the ith GPS signal incident on the antenna array from direction (θ_i, φ_i):

$$\mathbf{a}(\theta_i, \varphi_i) = \begin{bmatrix} a_{1H}(\theta_i, \varphi_i) & a_{1V}(\theta_i, \varphi_i) & \cdots & a_{NH}(\theta_i, \varphi_i) & a_{NV}(\theta_i, \varphi_i) \end{bmatrix}^H, \quad (11)$$

$\mathbf{A}_I(\rho, \phi)$ represents the interference $2N$-by-M steering matrix

$$\mathbf{A}_I(\rho, \phi) = \begin{bmatrix} \mathbf{a}(\rho_1, \phi_1) & \mathbf{a}(\rho_2, \phi_2) & \cdots & \mathbf{a}(\rho_M, \phi_M) \end{bmatrix}. \quad (12)$$

In the above equation, $\mathbf{a}(\rho_i, \phi_i)$ is the $2N$-by-1 steering vector of the ith interference

$$\mathbf{a}(\rho_i, \phi_i) = \begin{bmatrix} a_{1H}(\rho_i, \phi_i) & a_{1V}(\rho_i, \phi_i) & \cdots & a_{NH}(\rho_i, \phi_i) & a_{NV}(\rho_i, \phi_i) \end{bmatrix}^H. \quad (13)$$

The received signal vector $\mathbf{x}$(k) is the superposition of the GPS signals, interference, and AWGN noise:

$$\mathbf{x}(k) = \mathbf{A}_D(\theta)\mathbf{s}_D(k) + \mathbf{A}_I(\theta)\mathbf{i}_M(k) + \mathbf{n}(k), \quad (14)$$

where the $2N$-by-1 vector $\mathbf{n}$(k) represents the AWGN noise at the $2N$ antenna elements. The steering vector $\mathbf{a}(\theta, \varphi)$ at the UCA for linear-polarized signal from elevation angle θ, azimuth angle φ is expressed as

$$\mathbf{a}(\theta, \varphi) = \left\lfloor e^{j\varsigma \cos(\varphi - \varphi_1)}, e^{j\varsigma \cos(\varphi - \varphi_2)}, e^{j\varsigma \cos(\varphi - \varphi_N)} \right\rfloor, \quad (15)$$

where $\varsigma = kd \sin\theta$, and the angular position of the nth element of the array is given by

$$\phi_n = 2\pi\left(\frac{n}{N}\right), \quad n = 1, 2, \ldots, N. \quad (16)$$

Here, the wave number $k = 2\pi/\lambda$, where λ represents the wavelength. Assuming omnidirectional antennas, the steering vector for RHCP signal can be expressed as

$$\mathbf{a}(\theta_i, \varphi_i) = \begin{bmatrix} 1 & -j & \cdots & e^{j\varsigma \cos(\varphi_i - \varphi_N)} & -je^{j\varsigma \cos(\varphi_i - \varphi_N)} \end{bmatrix}^H, \quad (17)$$

where $a_{iV} = -ja_{iH}$. It is noted that for a horizontally polarized interference, $a_{iV} = 0$ $(i = 1, 2, \ldots, N)$, whereas for a vertically polarized interference, $a_{iH} = 0$ $(i = 1, 2, \ldots, N)$, and for LHCP interference, $a_{iV} = ja_{1H}$ $(i = 1, 2, \ldots, N)$.

3. ADAPTIVE MULTIPLE MVDR TECHNIQUE

3.1. Single MVDR beamformer technique

When minimizing the output power under unit-gain constraints toward all satellites, the array weights must satisfy

$$\min_{w} \mathbf{w}^H \mathbf{R} \mathbf{w} \text{ subject to } \mathbf{C}^H \mathbf{w} = \mathbf{f}, \quad (18)$$

where the constraint matrix $\mathbf{C}$ represents the GPS steering matrix $\mathbf{A}_D(\theta, \varphi)$, $\mathbf{f}$ is a D-by-1 vector of unit values, $\mathbf{f} = [1 \ 1 \ \cdots \ 1]^T$, and $\mathbf{R}$ represents the data spatial covariance matrix of the received data samples given by

$$\mathbf{R} = E[\mathbf{x}(k)\mathbf{x}^H(k)], \quad (19)$$

where $E[\cdot]$ denotes expectation. In practice, $\mathbf{R}$ is replaced by its estimates $\hat{\mathbf{R}}$:

$$\hat{\mathbf{R}} = \frac{1}{T}\sum_{i=1}^{T} \mathbf{x}(k)\mathbf{x}^H(k), \quad (20)$$

where T denotes the number of snapshots used in time-averaging covariance matrix estimation. The optimal weights for the above constrained minimization problem can be obtained as

$$\mathbf{w}_{\text{opt}} = \mathbf{R}^{-1}\mathbf{C}\left(\mathbf{C}^{H}\mathbf{R}^{-1}\mathbf{C}\right)^{-1}\mathbf{f}. \tag{21}$$

3.2. Multiple MVDR beamformer technique

Unlike the receiver shown in Figure 1, where only one set of weights is used to form a beamformer that satisfies all unit-gain constraints, the multiple MVDR beamforming technique generates several weight vectors, each corresponding to a beamformer toward one GPS satellite. Consequently, with D GPS satellites considered in the field of view, D sets of weight vectors are produced, where each set of weights maintains a unit-gain toward the direction of one GPS satellite, and places nulls toward all directions of jammers, irrespective of their temporal characteristics. The block diagram of multiple MVDR beamformers is shown in Figure 2. For the ith beamformer, the output power is minimized under the unit-gain constraint of the ith satellite, and is expressed as

$$\min_{w} \mathbf{w}_i^{H}\mathbf{R}\mathbf{w}_i \text{ subject to } \mathbf{c}_i^{H}\mathbf{w}_i = 1. \tag{22}$$

The optimum weight vector for the ith beamformer obtained from the above constraint minimizing problem is expressed as

$$\mathbf{w}_{i\_\text{opt}} = \mathbf{R}^{-1}\mathbf{c}_i\left(\mathbf{c}_i^{H}\mathbf{R}^{-1}\mathbf{c}_i\right)^{-1}, \tag{23}$$

where $\mathbf{c}_i$ represents the steering vector of the ith GPS signal, which is $\mathbf{a}(\theta_i, \varphi_i)$ in this case. The array output for the ith beamformer is given by

$$y_i(k) = \mathbf{w}_{i\_\text{opt}}^{H}\mathbf{x}(k). \tag{24}$$

It is noted that with multiple MVDR beamforming method, only one unit-gain constraint is presented. The total number of degrees of freedom associated with N dual-polarized antenna array is $2N$. Each RHCP jammer requires two degrees of freedom to be cancelled. Therefore, up to N-1 RHCP jammers can be mitigated from the nulls placed by the array spatial response. On the other hand, if all the jammers are LHCP, they can be directly cancelled by the array RHCP polarization property, that is, when using RHCP antennas. If the jammers are linearly polarized, up to N-1 linearly polarized jammers can be cancelled by the array spatial nulling based on the horizontal element weights. However, if the number of horizontally or vertically polarized jammers is more than N-1, the array will employ its dual-polarization property to set the corresponding weights to zero, and, in this way, it can cancel all jammers. These array properties are derived in the appendix. If the polarization characteristics of the jammers are the combination of the RHCP, LHCP, and linearly polarized, the array will apply both the spatial nulling and the polarization property in order to mitigate as much interference as possible. From the appendix and the above discussion, the following observations are in order. (a)

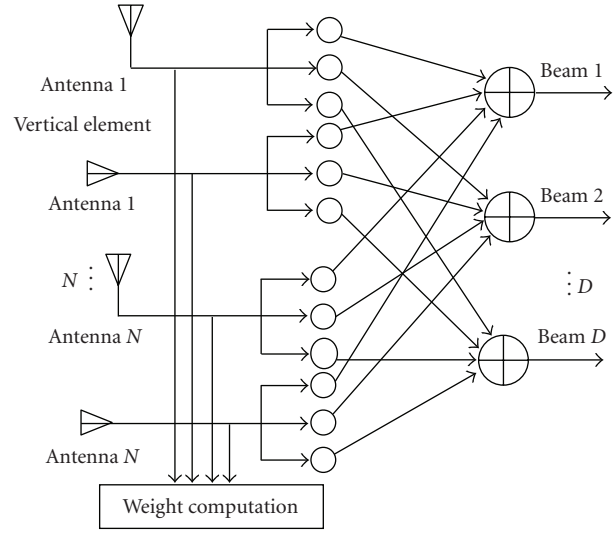

Figure 2: Block diagram of the multiple MVDR technique.

The array utilizes its RHCP polarization property to cancel a large number, or an infinite number of LHCP jammers. In addition to such cancellation, up to N-1 jammers with a combination of RHCP, vertical polarization, and horizontal polarization can be suppressed by the spatial nulling. (b) Up to N-1 jammers of a combination of RHCP and horizontal (vertical) polarization can be cancelled by spatial nulling along with a large number, or infinite number of vertically (horizontally) polarized jammers, which are cancelled by the array polarization property. In this respect, all the corresponding horizontal or vertical weights of the antenna array are zero, and half of the RHCP signal power is lost.

Another significant advantage of the multiple MVDR beamforming technique over other widely used techniques is that it can achieve regular array patterns upon jammer cancellation if the DOA of a jammer is close to or aligned with one of the GPS satellites. In this case, when using a single MVDR method, the array pattern becomes highly irregular. In consequence, the jammer that is aligned with the satellite will not be mitigated. Further, due to irregular pattern, the GPS receiver becomes vulnerable to newly borne jammers or on-off jammers with long duty cycles which may arrive from directions toward which the array places high irregular lobes. In comparison, in the multiple MVDR beamforming method, only the beamformer for which the satellite is close to the jammer is compromised, but the other D-1 beamformers remain intact with regular array patterns. In this respect, with typically more than four GPS satellites in the field of view, losing one GPS satellite information is not detrimental to the receiver pseudorange estimate calculations in signal acquisition and positioning tracking.

3.3. Adaptive implementation of multiple MVDR beamformer

Data covariance matrix estimation can be avoided if the weight vectors are calculated adaptively using constraint

Table 1: Summary of the simulation parameters.

Simulation subsections	Total no. of jammers	No. of RHCP jammers	No. of LHCP jammers	No. of vertically polarized jammers	No. of horizontally polarized jammers
4.1	4	4	0	0	0
4.2	8	4	0	2	2
4.3	10	0	0	10	0
4.4	2	2	0	0	0

LMS algorithm based on the received data samples. As a gradient-descent algorithm, constraint LMS algorithm iteratively adapts the weights of the antenna array such that the output power is minimized while the signal power is maintained at the receiver. The multiple MVDR beamforming method solves for $\mathbf{w}$ according to (23), which is rewritten here as

$$\min_{w} \mathbf{w}_i^H \mathbf{R}\mathbf{w}_i \text{ subject to } \mathbf{c}_i^H \mathbf{w}_i = 1. \tag{25}$$

Denote $\mathbf{F}_i = \mathbf{c}_i(\mathbf{c}_i^H\mathbf{c}_i)^{-1}$ and $\mathbf{P}_i = \mathbf{I} - \mathbf{c}_i(\mathbf{c}_i^H\mathbf{c}_i)^{-1}\mathbf{c}_i^H$. The weight vector for the ith beamformer can be recursively updated as [26]

$$\begin{aligned}\mathbf{w}_i(k+1) &= \mathbf{P}_i\mathbf{w}_i(k) - \mu\mathbf{P}_i\mathbf{R}\mathbf{w}_i(k) + \mathbf{F}_i \\ &= \mathbf{P}_i(\mathbf{w}_i(k) - \mu\mathbf{R}\mathbf{w}_i(k)) + \mathbf{F}_i \\ &= \mathbf{P}_i(\mathbf{w}_i(k) - \mu y_i(k)\mathbf{x}(k)) + \mathbf{F}_i,\end{aligned} \tag{26}$$

where μ is the adaptation step size, satisfying $0 < \mu < 2/3\text{tr}(\mathbf{R})$. Initially, $\mathbf{w}(0) = \mathbf{F}_0$. The output power of the antenna array of the ith beamformer is $\mathbf{w}_i^H\mathbf{R}\mathbf{w}_i$. Details of the derivations of (25)-(26) can be found in [26].

4. SIMULATIONS

In this section, we present simulations for various jamming situations, where different number of jammers, different polarization characteristics of narrowband jammers, and different directions of jammers are involved. The array weight vectors are obtained adaptively using constraint LMS algorithm. The performances of single MVDR and multiple MVDR beamformers are presented and compared. Eight dual-polarized antennas are uniformly distributed in a circle with the radius of half the wavelength. The range of elevation angle is from zero to 180 degrees and the range of azimuth angle is from zero to 360 degrees. Four GPS satellites in the field of view are incident on the antenna array from elevation angles of 30, 60, 80, and 120 degrees and azimuth angles of 150, 80, 330, and 220 degrees, respectively, with a signal-to-noise ratio (SNR) of −20 dB. The number of snapshot is set to 1000. Table 1 summarizes the values assumed by the different variables in the subsequent simulations. All jammers are modeled as white noise with the same bandwidth as the GPS signal.

4.1. RHCP jammers only

In this simulation, four RHCP jammers impinge on the antenna array from elevation angles of 10, 40, 140, and 170 degrees, and azimuth angles of 100, 300, 40, and 190 degrees are considered with a jammer-to-noise ratio (JNR) of 20 dB. These jammers are numbered respectively as jammer 1, 2, 3, 4. The step size of the constraint LMS algorithm is set to 0.00005. Figure 3(a) represents the interference cancellation performance upon convergence with adaptive single MVDR beamforming method. Figure 3(b) depicts the performances of all beamformers of the multiple MVDR beamforming method. The "$*$" indicates the positions of the jammers, whereas the circles indicate the positions of the satellites. The corresponding array outputs at the directions of the four jammers are −15, −8, −7, and −12 dB, respectively, with single MVDR beamforming method. In comparison, the array outputs at these jammers' directions using the adaptive multiple MVDR beamformers are below −40 dB. It is clear that the single MVDR beamforming method is not able to cancel the four jammers, since only up to three jammers can be cancelled due to the available degrees of freedom. Figure 4 illustrates the cross-correlation of one of the received GPS signals, after applying beamforming, with the corresponding receiver local codes. We used one of the 24 GPS satellite codes. It is clear that the correlation has high peak at zero point with multiple MVDR beamforming method, while it is randomly distributed with the single MVDR beamformer method.

Figure 5 shows the array output powers as a function of time for each beamformer of the multiple MVDR beamforming method and single MVDR. For the same step size parameter value, three multiple MVDR beamformers clearly converge faster than the single MVDR beamformer. This is a result of variations in the error surface among the beamformers. The convergence performance, however, is generally guided by the dimension of the error surface and can favor the single MVDR beamforming due to fewer degrees of freedom.

4.2. Combination of RHCP, vertically polarized, and horizontally polarized jammers

In addition to the four RHCP jammers discussed in the previous section, we consider two horizontally polarized jammers arrive from elevation angles of 20 and 50 degrees and azimuth angles of 200 and 120 degrees, respectively, with 20 dB JNR, and two vertically polarized jammers arrive from elevation angles of 100 and 160 degrees and azimuth angles of 260 and 10 degrees, respectively, with the 20 dB JNR. The step size remains at 0.00005.

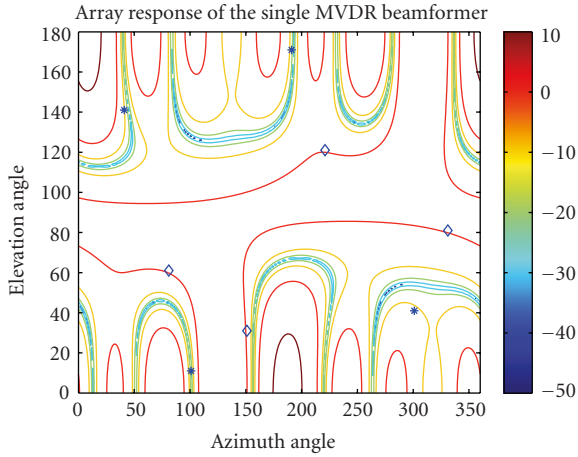

(a)

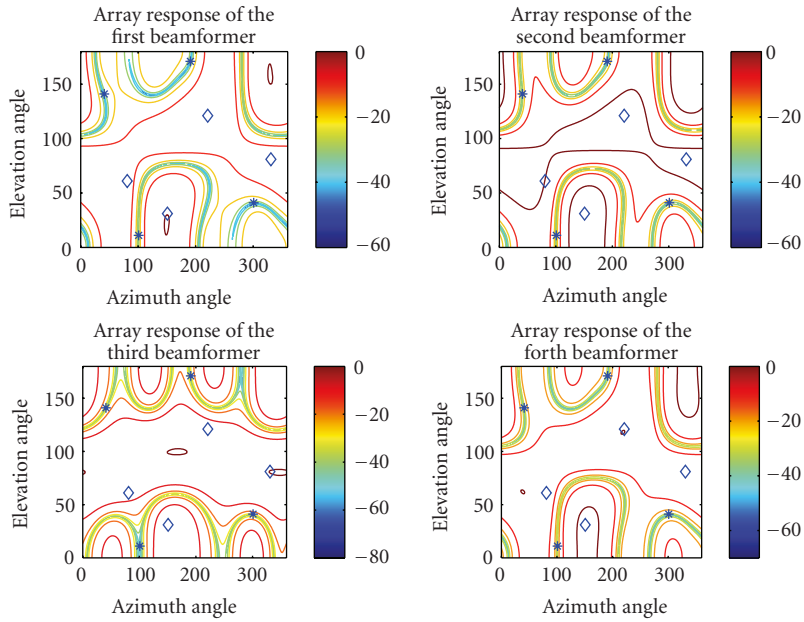

(b)

Figure 3: (a) Array response of the single-adaptive MVDR beamformer with four RHCP jammers. (b) Array response of the adaptive multiple MVDR beamformers with four RHCP jammers.

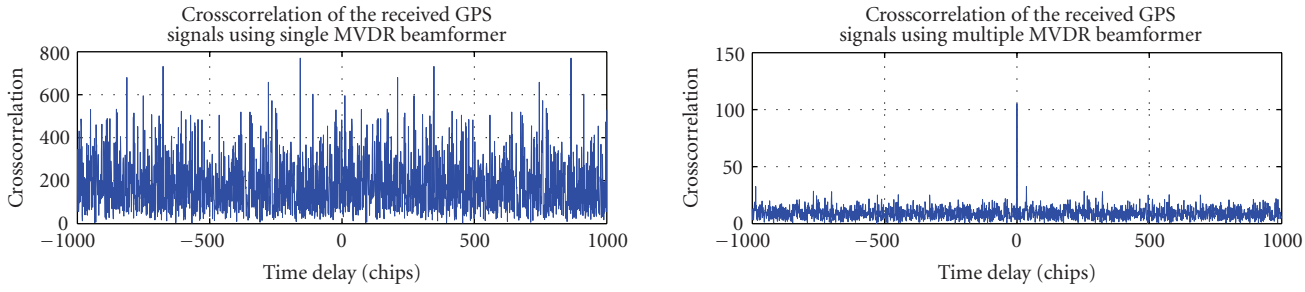

(a) (b)

Figure 4: Cross-correlation of the received GPS for single and the first beamformer of the multiple MVDR beamformers with four RHCP jammers.

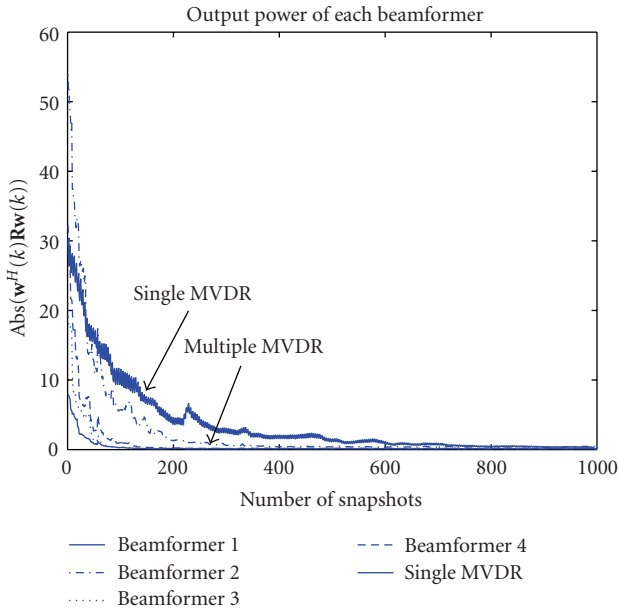

FIGURE 5: Output power of the LMS algorithm at each beamformer.

Figure 6(a) represents the RHCP interference cancellation performance with adaptive multiple MVDR beamforming method upon convergence, Figure 6(b) shows the array performance toward the vertically polarized jammers for each beamformer of the multiple MVDR beamforming method, and Figure 6(c) demonstrates the array performance for horizontally polarized jammers for each beamformer. It is evident that the array outputs at the directions of the jammers for all the three polarizations are below −40 dB. Figure 7 depicts the cross-correlation function of the received GPS signals with the local codes for single and multiple MVDR methods. The received GPS signal and the local code are assumed to be synchronized, that is, acquisition is maintained. Only the cross-correlation of the first beamformer, corresponding to the satellite of (azimuth, elevation) = (30, 120) degrees, in the multiple MVDR method, is displayed. It is clear that the single-beamformer receiver fails to produce a peak at zero lag, whereas in using multiple MVDR method, the correlation has a clear high peak.

4.3. *Large number of vertically polarized jammers*

We consider ten vertically polarized jammers arriving from elevation angles of 10, 40, 140, 170, 20, 50, 100, 160, 170, and 130 degrees and azimuth angles of 100, 300, 40, 190, 200, 120, 260, 10, 290, and 60 degrees, respectively, with JNRs of 20 dB. The step size is set to 0.00005. This value is consistent with the convergence and imposed by the trace of the covariance matrix.

Figure 8 demonstrates the vertically polarized interference cancellation performance with adaptive multiple MVDR beamforming method upon convergence. Since the number of vertically polarized jammers exceeds the number of available degrees of freedom, the dual-polarized antenna array employs the polarization property rather than coherent array processing to cancel the jammers. The array response at any direction is less than −40 dB for any vertical signal.

4.4. *A RHCP jammer aligned with the direction of one GPS satellite*

This section examines the scenario when two RHCP jammers arrive from elevation angles of 10 and 80 degrees and azimuth angles of 100 and 330 degrees, respectively. The second jammer is from the same direction as one of the satellites. Figure 9(a) depicts the cancellation performance of a single MVDR beamformer, where the array outputs at the two jammers' directions are −44 and 0 dB. Constraint minimization requires the single MVDR beamformer to keep unit-gain at the direction of the satellite, permitting the GPS signal along with the second interference to be received with equal sensitivity. Figure 9(b) shows the performance for each beamformer of the multiple MVDR beamforming method. The array responses at the two jammers' directions for the four beamformers are −45 and −48 dB, −49 and −62 dB, −53 and 0 dB, −51 and −50 dB, respectively. Based on the simulation results in Figures 9(a) and 9(b), with the exception of the beamformer for which the satellite is aligned in angle with the jammer, all other three beamformers successfully suppress the interference and provide the correct position tracking information.

Table 2 shows the reduction of noise and jammer power as the input data are processed by the beamformer. We consider beamformers 1 and 2. The table also depicts the BER using the optimum beam weight vector and based on the BFSK probability of error expressions with Gaussian noise. Recall that the jammers used are white noise signals and can be considered as part of the overall added noise the GPS signal coming into the receiver correlator. Both BER values with and without the beamformer are stated. The effect of the spreading gain (approx., 30 dB) on BER is delineated. It is clear that the dual-polarized multiple MVDR beamforming significantly reduces the BER as compared to a single antenna receiver. This is attributed to the strong nulling performance of the dual polarize array for each jammer. Only for the beamformer in which the jammer is very close to or shares the angular position with one of the GPS in the field of view, the BER performance is compromised.

5. CONCLUSIONS

This paper analyzed the interference cancellation performance at the GPS receiver using uniform circular dual-polarized antenna array. The adaptive multiple MVDR beamforming method was employed to recursively update the weigh vector associated with each satellite. One advantage of using dual-polarized antenna array at the receiver is its ability to handle different polarization characteristics of the interference. Any LHCP jammer or a large number of linearly polarized jammers can be cancelled by the polarization property of the dual-polarized antenna. The adaptive multiple MVDR beamforming method has additional degrees of freedom compared with the single MVDR beamforming

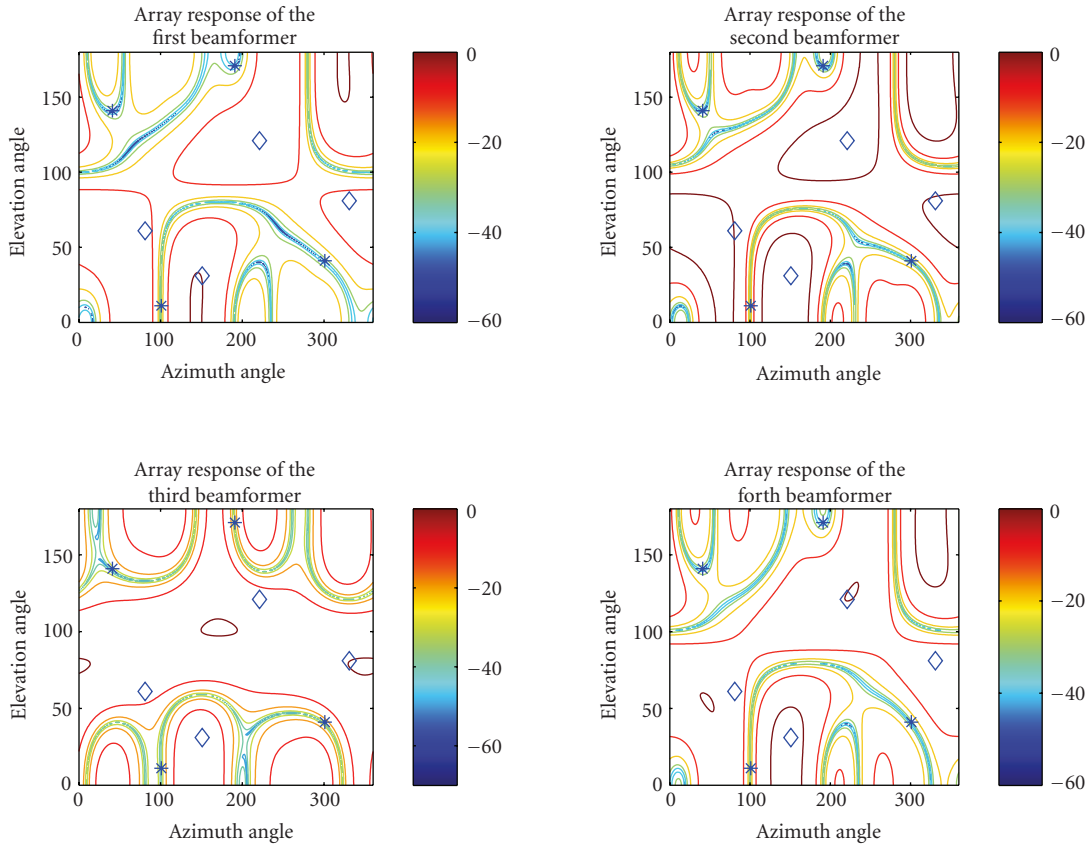
Array response of the first beamformer
Array response of the second beamformer
Array response of the third beamformer
Array response of the forth beamformer
Elevation angle
Azimuth angle
0
50
100
150
0
100
200
300
0
−20
−40
−60

(a)

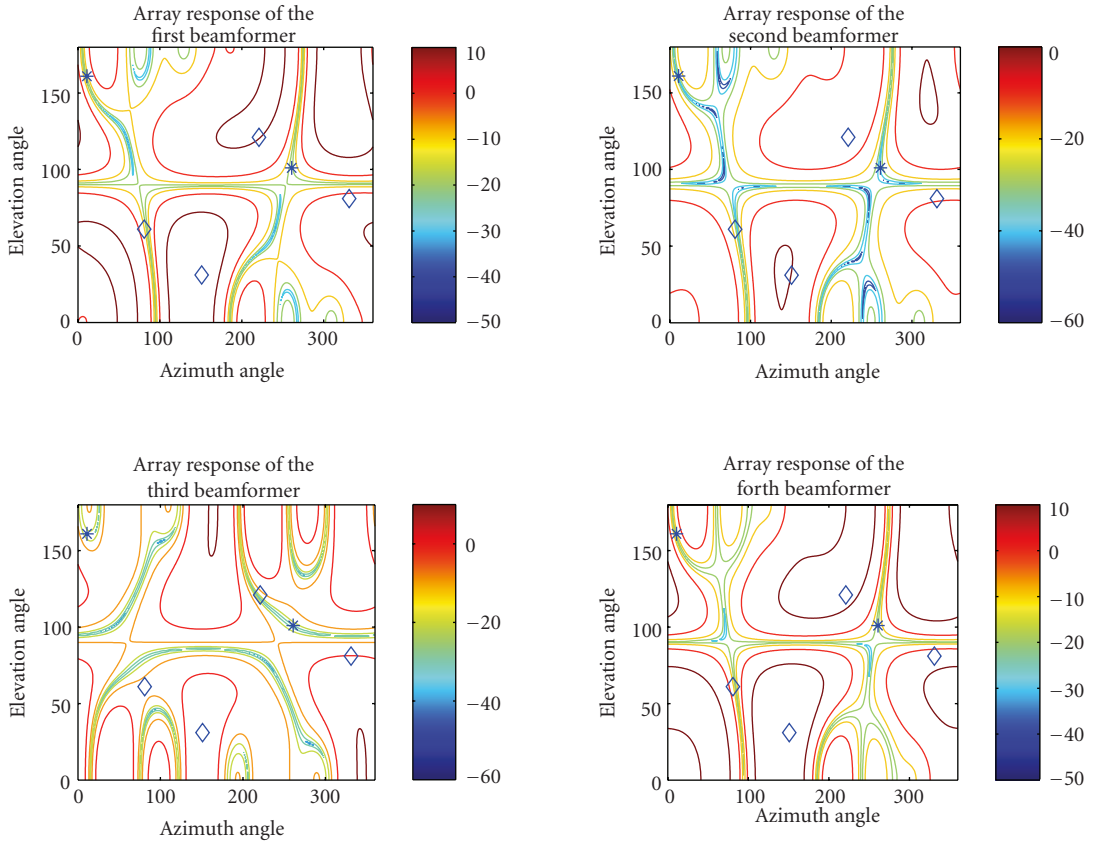
Array response of the first beamformer
Array response of the second beamformer
Array response of the third beamformer
Array response of the forth beamformer
Elevation angle
Azimuth angle
0
50
100
150
0
100
200
300
10
0
−10
−20
−30
−40
−50
−60

(b)

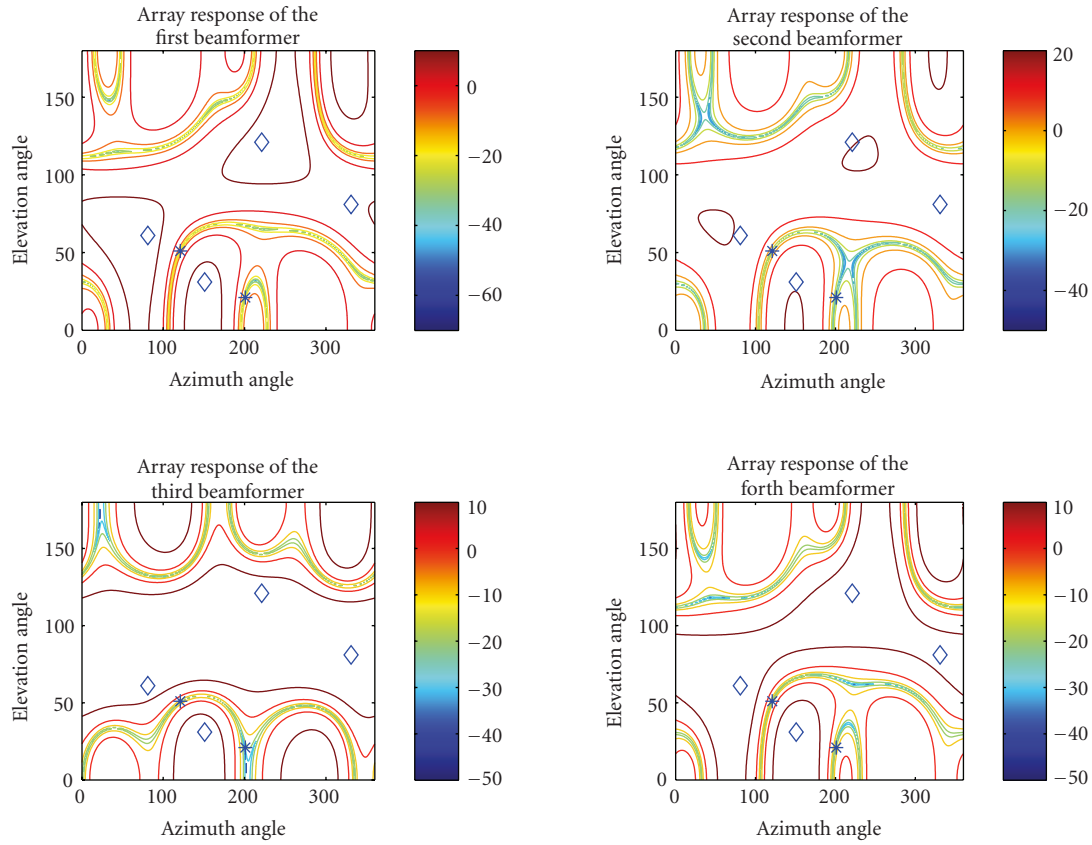

(c)

Figure 6: (a) Array response of the adaptive multiple MVDR beamformers with four RHCP jammers. (b) Array response of the adaptive multiple MVDR beamformers with two vertically polarized jammers. (c) Array response of the adaptive multiple MVDR beamformers with two horizontally polarized jammers.

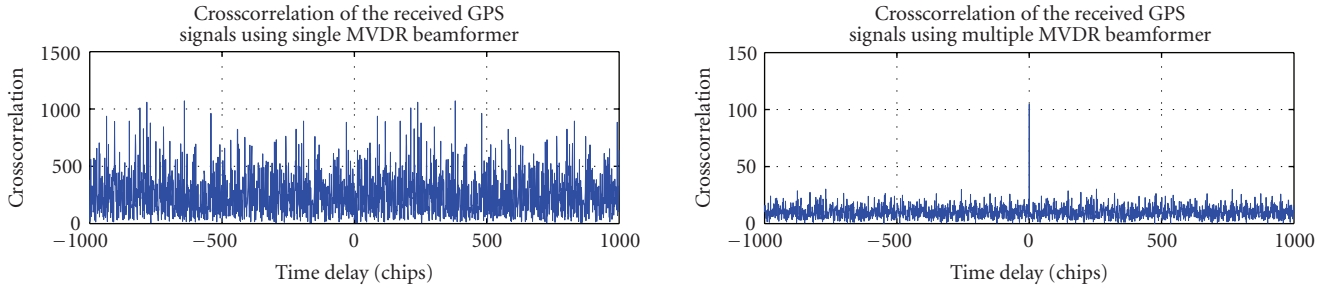

(a) (b)

Figure 7: Cross-correlation of the received GPS for single and the first beamformer of the multiple MVDR beamformers with four RHCP jammers.

method. The combination of the polarization and excess degrees of freedom renders jammer cancellation more effective. Specifically, one clear advantage of the multiple MVDR beamforming approach is that it sustains the nulling performance of the receiver array when jammers are close to or align in angle to GPS satellites. This situation is very challenging to the single MVDR beamforming approach and will cause loss of acquisition for all satellites in the field of view. When the polarization property is used to cancel a large number of LHCP, vertically polarized or horizontally polarized jammers, up to N-1 jammers with the combination of other polarization characteristics, can be eliminated with the adaptive array processing.

This paper also examined the situation when the jammer is aligned in angle with or close to one GPS satellite. Only the beamformer that is associated with the direction of the jammer fails to cancel the interference and provides irregular array pattern. As more than four satellites are typically found

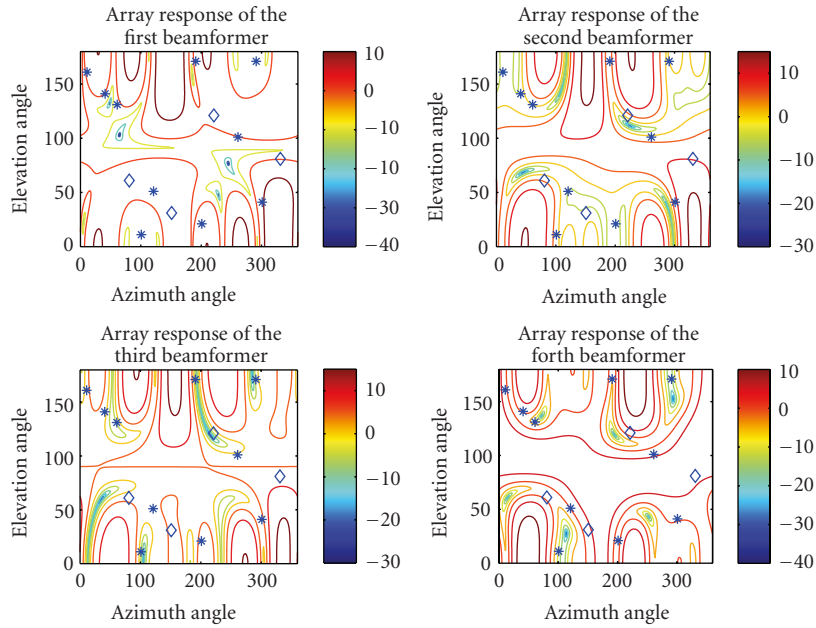

Figure 8: Array response of the adaptive multiple MVDR beamformers with ten vertically polarized jammers.

Table 2: Jammer cancellation data and BER for beamfomers 1and 2.

Simulation subsections	4.1	4.2	4.3	4.4	
Beamformer	1	1	1	1	3 (align with jammer)
Input JSR	40 dB	40 dB	40 dB	40 dB	40 dB
Total number of jammers	4	8	10	2	2
Output JSR(dB)	−37, −13, −27, −13	−23, −22, −15, −38, −22, −25, −18, −32	−37, −28, −15, −21, −31, −37, −15, −52, −20, −26	−31, −21	7, 37
Output SNR	−8 dB	−11 dB	−11 dB	−9 dB	−21 dB
Output SINR	−8 dB	−11 dB	−11 dB	−9 dB	−37 dB
BER	0.2867	0.3451	0.3451	0.3079	0.4920
BER considering spreading gain	3e−071	1e−036	1e−036	5e−057	0.2638
BER without beamformer	0.4944	0.4944	0.4944	0.4944	0.4944
Beamformer	2	2	2	2	
Input JSR	40 dB	40 dB	40 dB	40 dB	
Total number of jammers	4	8	10	2	
Output JSR(dB)	−22, −22, −14, −42	−7, −5, −27, −6, −35, −35, −20, −7	−12, −22 −34, −26, −22, −16, −24, −15, −25, −11	−15, −39	
Output SNR	−14 dB	−17 dB	−11 dB	−10 dB	
Output SINR	−14 dB	−17 dB	−11 dB	−10 dB	
BER	0.3889	0.4208	0.3451	0.3274	
BER considering spreading gain	2.3e−19	1.3e−10	1e−36	1e−45	
BER without beamformer	0.4944	0.4944	0.4944	0.4944	

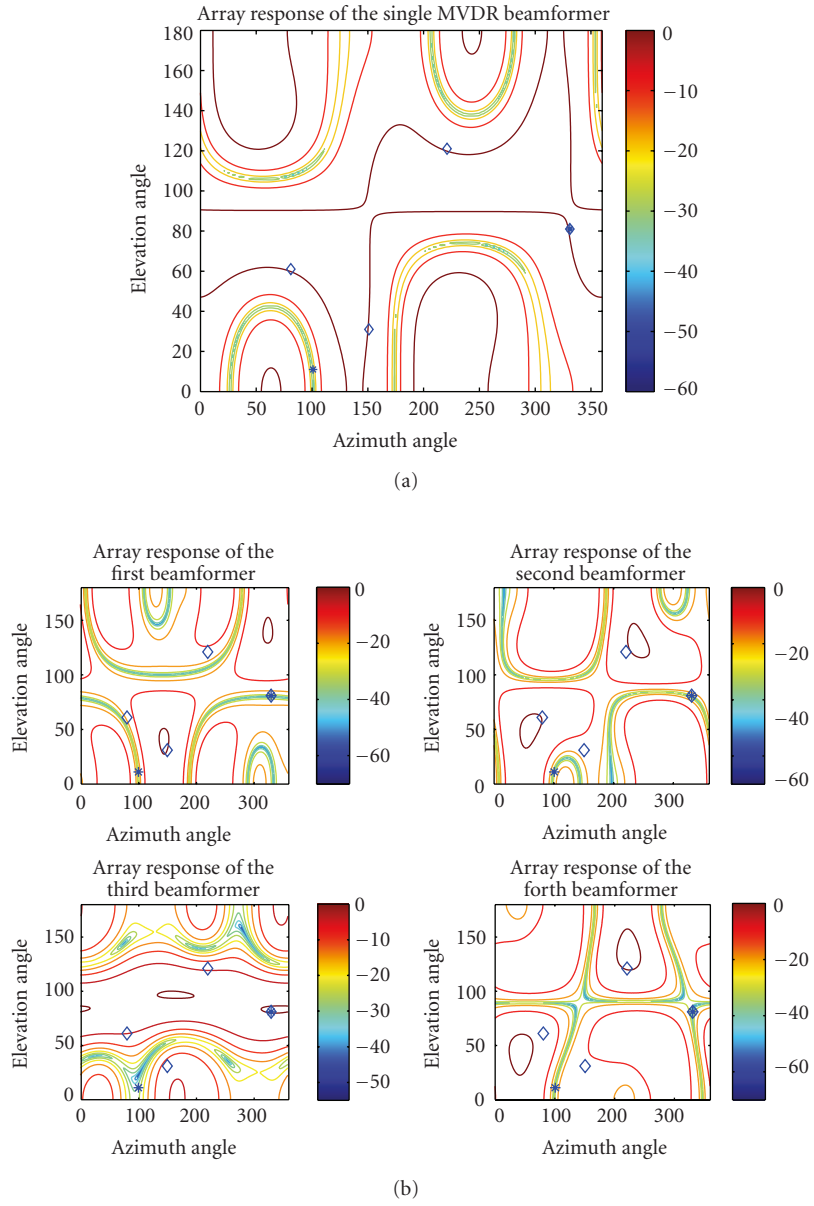

FIGURE 9: (a) Array response of the adaptive single MVDR beamformers with two RHPC jammers where one is aligned with one of the GPS satellites. (b) Array response of the adaptive multiple MVDR beamformers with two RHPC jammers where one is aligned with one of the GPS satellites.

in the filed of view of a GPS receiver, the compromise is not detrimental to the receiver pseudorange estimate calculations in signal acquisition and positioning tracking.

APPENDIX

The covariance matrix $\mathbf{R}$ in (19) can be written as

$$\mathbf{R} = \mathbf{x}\mathbf{x}^H = \sum_{i=1}^{D} P_{Si}\mathbf{a}(\theta_i,\varphi_i)\mathbf{a}^H(\theta_i,\varphi_i) + \sum_{i=1}^{M} P_{Ii}\mathbf{a}(\rho_i,\phi_i)\mathbf{a}^H(\rho_i,\phi_i) + \sigma_n^2\mathbf{I}, \tag{A.1}$$

where P_{Si} represents the signal power from the ith satellite, P_{Ii} represents the power of the ith interferer, and σ_n^2 represents the noise power. It is noted that the first term in (A.1) is negligible due to the low power of the GPS signals. Therefore, the data covariance matrix $\mathbf{R}$ can be simplified as

$$\mathbf{R} = \sum_{i=1}^{M} P_{Ii}\mathbf{a}(\rho_i,\phi_i)\mathbf{a}^H(\rho_i,\phi_i) + \sigma_n^2\mathbf{I} = \mathbf{P} + \sigma_n^2\mathbf{I}. \tag{A.2}$$

If the jammers are vertically polarized, the steering vector $\mathbf{a}(\rho_i,\phi_i)$ is characterized by $a_{iH} = 0$ $(i = 1,2,\ldots,N)$, and

thus, the matrix $\mathbf{P}$ has zero values at all elements in the odd rows and the odd columns. Accordingly,

$$R=\begin{bmatrix} \sigma_n^2 & 0 & 0 & 0 & 0 & \cdots & 0 & 0 \\ 0 & p_{22}+\sigma_n^2 & 0 & p_{24} & 0 & \cdots & 0 & p_{2,2N} \\ 0 & 0 & \sigma_n^2 & 0 & 0 & \cdots & 0 & 0 \\ 0 & p_{42} & 0 & p_{44}+\sigma_n^2 & 0 & \cdots & 0 & p_{4,2N} \\ 0 & 0 & 0 & 0 & \sigma_n^2 & \cdots & 0 & 0 \\ \cdots & \cdots & \cdots & \cdots & \cdots & \cdots & \cdots & \cdots \\ 0 & 0 & 0 & 0 & 0 & \cdots & \sigma_n^2 & 0 \\ 0 & p_{2N,2} & 0 & p_{2N,4} & 0 & \cdots & 0 & p_{2N,2N}+\sigma_n^2 \end{bmatrix}, \tag{A.3}$$

where p_{ij} denotes the element at row i, column j in the matrix $\mathbf{P}$. Applying eigendecomposition, the eigenvalues λ satisfy

$$\det\begin{bmatrix} \mathcal{A} & 0 & 0 & 0 & 0 & \cdots & 0 & 0 \\ 0 & \mathcal{B}+\mathcal{A} & 0 & p_{24} & 0 & \cdots & 0 & p_{2,2N} \\ 0 & 0 & \mathcal{A} & 0 & 0 & \cdots & 0 & 0 \\ 0 & \mathcal{C} & 0 & \mathcal{F}+\mathcal{A} & 0 & \cdots & 0 & p_{4,2N} \\ 0 & 0 & 0 & 0 & \mathcal{A} & \cdots & 0 & 0 \\ \cdots & \cdots & \cdots & \cdots & \cdots & \cdots & \cdots & \cdots \\ 0 & 0 & 0 & 0 & 0 & \cdots & \mathcal{A} & 0 \\ 0 & \mathcal{D} & 0 & p_{2N,4} & 0 & \cdots & 0 & \mathcal{E}+\mathcal{A} \end{bmatrix} = 0, \tag{A.4}$$

where $\mathcal{A}$ denotes $\sigma_n^2-\lambda$, $\mathcal{B}$ denotes p_{22}, $\mathcal{C}$ denotes p_{42} , $\mathcal{D}$ denotes $p_{2N,2}$, $\mathcal{E}$ denotes $p_{2N,2N}$, and $\mathcal{F}$ denotes p_{44}.

The determinant of the matrix can be expressed as

$$(\sigma_n^2-\lambda)^N \det \times \begin{bmatrix} p_{22}+\sigma_n^2-\lambda & p_{24} & \cdots & p_{2,2N} \\ p_{42} & p_{44}+\sigma_n^2-\lambda & \cdots & p_{4,2N} \\ \cdots & \cdots & \cdots & \cdots \\ p_{2N,2} & p_{2N,4} & \cdots & p_{2N,2N}+\sigma_n^2-\lambda \end{bmatrix} = 0. \tag{A.5}$$

It is easy to see that at least N eigenvalues are equal to the noise power σ_n^2, and their corresponding eigenvectors satisfy

$$\begin{bmatrix} 0 & 0 & 0 & 0 & 0 & \cdots & 0 & 0 \\ 0 & p_{22} & 0 & p_{24} & 0 & \cdots & 0 & p_{2,2N} \\ 0 & 0 & 0 & 0 & 0 & \cdots & 0 & 0 \\ 0 & p_{42} & 0 & p_{44} & 0 & \cdots & 0 & p_{4,2N} \\ 0 & 0 & 0 & 0 & 0 & \cdots & 0 & 0 \\ \cdots & \cdots & \cdots & \cdots & \cdots & \cdots & \cdots & \cdots \\ 0 & 0 & 0 & 0 & 0 & \cdots & 0 & 0 \\ 0 & p_{2N,2} & 0 & p_{2N,4} & 0 & \cdots & 0 & p_{2N,2N} \end{bmatrix} \begin{bmatrix} e_1 \\ e_2 \\ \cdots \\ e_{2N} \end{bmatrix} = 0. \tag{A.6}$$

Define

$$\widetilde{\mathbf{P}} = \begin{bmatrix} p_{22} & p_{24} & \cdots & p_{2,2N} \\ p_{42} & p_{44} & \cdots & p_{4,2N} \\ \cdots & \cdots & \cdots & \cdots \\ p_{2N,2} & p_{2N,4} & \cdots & p_{2N,2N} \end{bmatrix} \tag{A.7}$$

and $\widetilde{\mathbf{e}} = [e_2 \;\; e_4 \;\; \cdots \;\; e_{2N}]^T$, (A.6) can be written as

$$\widetilde{\mathbf{P}}\widetilde{\mathbf{e}} = \mathbf{0}. \tag{A.8}$$

Obviously, if the number of vertically polarized jammers is smaller than N, the rank of the matrix $\widetilde{\mathbf{P}}$ becomes M. Otherwise, the matrix $\widetilde{\mathbf{P}}$ has full rank N, and $\widetilde{\mathbf{e}} = \mathbf{0}$. Accordingly, the eigenvector $e_2, e_4, \ldots, e_{2N} = 0$, which means that these eigenvectors are horizontally polarized. The eigendecomposition of the data covariance matrix is

$$\mathbf{R} = \mathbf{E}\Lambda\mathbf{E}^H, \tag{A.9}$$

where Λ is the diagonal eigenvalue matrix, $\mathbf{\Lambda} = \text{diag}\{\sigma_1^2 \cdots \sigma_M^2\sigma_n^2 \cdots \sigma_n^2\}$, and $\mathbf{E}$ is the corresponding eigenvector matrix. In the above equation, σ_i^2 $(i = 1, 2, \ldots, M)$ represents the ith significant eigenvalue and σ_n^2 represents the noise eigenvalue. The eigendecomposition of the inverse of the data covariance matrix is expressed as

$$\mathbf{R}^{-1} = \mathbf{E}\mathbf{\Lambda}^{-1}\mathbf{E}^H = \sum_{i=1}^{M}\frac{1}{\sigma_i^2}\mathbf{e}_i\mathbf{e}_i^H + \sum_{j=M+1}^{2N}\frac{1}{\sigma_n^2}\mathbf{e}_j\mathbf{e}_j^H, \tag{A.10}$$

where $1/\sigma_i^2 \ll 1/\sigma_n^2$. It is obvious that if the number of vertically polarized jammers is greater than N, the noise eigenvectors are horizontally polarized, and thus, the weights obtained by (22) will be horizontally polarized. This implies that the array vertical polarization weights are zeros.

In the case that the jammers are the combination of RHCP and vertically polarized, for example, M_1 RHCP jammers and M_2 vertically polarized jammers, the data covariance matrix $\mathbf{R}$ in (A.2) can be written as,

$$\begin{aligned}\mathbf{R} &= \sum_{i=1}^{M_1} P_{Ii}\mathbf{a}(\rho_i,\varphi_i)\mathbf{a}^H(\rho_i,\varphi_i) + \sum_{j=1}^{M_2} P_{Ij}\mathbf{a}(\rho_j,\varphi_j)\mathbf{a}^H(\rho_j,\varphi_j) + \sigma_n^2\mathbf{I} \\ &= \mathbf{P}_1 + \mathbf{P}_2 + \sigma_n^2\mathbf{I},\end{aligned} \tag{A.11}$$

where $\mathbf{P}_2$ has the same structure as $\mathbf{P}$ in (A.2). When M_1 and M_2 are smaller than N, since the steering vectors involved in constructing $\mathbf{P}_1$ and $\mathbf{P}_2$ are linearly independent, $\mathbf{P}_1$ is a matrix of rank M_1, whereas the second matrix $\mathbf{P}_2$ has the rank M_2. However, if M_2 is larger than N, the rank of $\mathbf{P}_2$ is N, producing the rank of $\mathbf{P}_1+\mathbf{P}_2$ to be M_1+N. Therefore, $N-M_1$ eigenvalues of the matrix $\mathbf{R}$ are the noise eigenvalues, and their corresponding eigenvectors are horizontally polarized, as we stated before. Taking the eigendecomposition of the inverse of $\mathbf{R}$, (A.10) then will be the linear combination of those noise eigenvectors, leading to the corresponding vertical weight elements to be of zero values.

ACKNOWLEDGMENTS

This work is sponsored in part by NSF, Grant no. EEC-0332490, and in part by ONR, Contract no. N65540-05-C-0028.

REFERENCES

[1] M. S. Grewal, L. R. Weill, and A. P. Andrews, *Global Positioning Systems, Inertial Navigation, and Integration*, John Wiley & Sons, New York, NY, USA, 2001.

[2] W. Sun and M. G. Amin, "Interference suppression for GPS coarse/acquisition signals using antenna array," in *Proceedings of IEEE International Conference on Acoustics, Speech, and Signal Processing (ICASSP '04)*, vol. 4, pp. 929–932, Montreal, Canada, May 2004.

[3] J. W. Ketchum and J. G. Proakis, "Adaptive algorithms for estimating and suppressing narrow-band interference in PN spread-spectrum systems," *IEEE Transactions on Communications*, vol. 30, no. 5, part 2, pp. 913–924, 1982.

[4] L. B. Milstein, "Interference rejection techniques in spread spectrum communications," *Proceedings of the IEEE*, vol. 76, no. 6, pp. 657–671, 1988.

[5] K. Deergha Rao and M. N. S. Swamy, "New approach for suppression of FM jamming in GPS receivers," *IEEE Transactions on Aerospace and Electronic Systems*, vol. 42, no. 4, pp. 1464–1474, 2006.

[6] B. Badke and A. S. Spanias, "Partial band interference excision for GPS using frequency-domain exponents," in *Proceedings of IEEE International Conference on Acoustics, Speech, and Signal Processing (ICASSP '02)*, vol. 4, pp. 3936–3939, Orlando, Fla, USA, May 2002.

[7] P. T. Capozza, B. J. Holland, T. M. Hopkinson, and R. L. Landrau, "A single-chip narrow-band frequency-domain excisor for a Global Positioning System (GPS) receiver," *IEEE Journal of Solid State Circuits*, vol. 35, no. 3, pp. 401–411, 2000.

[8] R. C. DiPietro, "An FFT based technique for suppressing narrow-band interference in PN spread spectrum communications systems," in *Proceedings of IEEE International Conference on Acoustics, Speech, and Signal Processing (ICASSP '89)*, vol. 2, pp. 1360–1363, Glasgow, UK, May 1989.

[9] Y. Zhang, A. R. Lindsey, and M. G. Amin, "Combined synthesis and projection techniques for jammer suppression in DS/SS communications," in *Proceedings of IEEE International Conference on Acoustics, Speech, and Signal Processing (ICASSP '02)*, vol. 3, pp. 2757–2760, Orlando, Fla, USA, May 2002.

[10] M. G. Amin, L. Zhao, and A. R. Lindsey, "Subspace array processing for the suppression of FM jamming in GPS receivers," *IEEE Transactions on Aerospace and Electronic Systems*, vol. 40, no. 1, pp. 80–92, 2004.

[11] H. Subbaram and K. Abend, "Interference suppression via orthogonal projections: a performance analysis," *IEEE Transactions on Antennas and Propagation*, vol. 41, no. 9, pp. 1187–1194, 1993.

[12] M. Trinkle and W. C. Cheuk, "Null-steering GPS dual-polarized antenna arrays," in *Proceedings of the 6th International Symposium on Satellite Navigation Technology including Mobile Positioning and Location Services (SatNav '03)*, Melbourne, Australia, July 2003.

[13] R. L. Fante and J. J. Vaccaro, "Evaluation of adaptive space-time-polarization cancellation of broadband interference," in *Proceedings of IEEE Position Location and Navigation Symposium (PLANS '02)*, pp. 1–3, Palm Springs, Calif, USA, April 2002.

[14] F. L. Fante and J. J. Vaccaro, "Jammer cancellation performance of a fully-polarimetric GPS array," Tech. Rep., MITRE, Bedford, Mass, USA, November 2001.

[15] G. Lachapelle, M. Petovello, L. Scott, S. Skone, and J. Raquet, "GNSS Solutions: adaptive antenna arrays, multi-GNSS tropospheric monitoring, and high-dynamic receivers," *Inside GNSS, Engineering Solutions for the Global Navigation Satellite System*, vol. 1, no. 3, pp. 20–25, 2006.

[16] G. Seco-Granados, J. A. Fernández-Rubio, and C. Fernández-Prades, "ML estimator and hybrid beamformer for multipath and interference mitigation in GNSS receivers," *IEEE Transactions on Signal Processing*, vol. 53, no. 3, pp. 1194–1208, 2005.

[17] M. D. Zoltowski and A. S. Gecan, "Advanced adaptive null steering concepts for GPS," in *Proceedings of IEEE Military Communications Conference (MILCOM '95)*, vol. 3, pp. 1214–1218, San Diego, Calif, USA, November 1995.

[18] M. Trinkle and D. Gray, "GPS interference mitigation; overview and experimental results," in *Proceedings of the 5th International Symposium on Satellite Navigation Technology & Applications (SatNav '01)*, Canberra, Australia, July 2001.

[19] Y. Zhang, M. G. Amin, and A. R. Lindsey, "Anti-jamming GPS receivers based on bilinear signal distributions," in *Proceedings of IEEE Military Communications Conference (MILCOM '01)*, vol. 2, pp. 1070–1074, McLean, Va, USA, October 2001.

[20] R. L. Fante and J. J. Vaccaro, "Wideband cancellation of interference in a GPS receive array," *IEEE Transactions on Aerospace and Electronic Systems*, vol. 36, no. 2, pp. 549–564, 2000.

[21] G. F. Hatke, "Adaptive array processing for wideband nulling in GPS systems," in *Proceedings of the 32nd Asilomar Conference on Signals, Systems and Computers*, vol. 2, pp. 1332–1336, Pacific Grove, Calif, USA, November 1998.

[22] P. Xiong, M. J. Medley, and S. N. Batalama, "Spatial and temporal processing for global navigation satellite systems: the GPS receiver paradigm," *IEEE Transactions on Aerospace and Electronic Systems*, vol. 39, no. 4, pp. 1471–1484, 2003.

[23] W. L. Myrick, S. Goldstein, and M. D. Zoltowski, "Low complexity anti-jam space-time processing for GPS," in *Proceedings of IEEE International Conference on Acoustics, Speech, and Signal Processing (ICASSP '01)*, vol. 4, pp. 2233–2236, Salt Lake, Utah, USA, May 2001.

[24] J. Wang and M. Amin, "GPS interference cancellation performance for single and multiple MVDR beamformers," in *Proceedings of the 40th Asilomar Conference on Signals, Systems and Computers*, Pacific Grove, Calif, USA, October-November 2006.

[25] M. G. Amin, "Concurrent nulling and locations of multiple interferences in adaptive antenna arrays," *IEEE Transactions on Signal Processing*, vol. 40, no. 11, pp. 2658–2668, 1992.

[26] O. L. Frost III, "An algorithm for linearly constrained adaptive array processing," *Proceedings of the IEEE*, vol. 60, no. 8, pp. 926–935, 1972.